UNIVERSITY OF CALIFORNIA, MERCED

Dipolar Bose-Einstein Condensate Dynamics in A Chaotic Potential

A thesis submitted in partial satisfaction of the requirements for the degree of

Master of Science

in

Physics

by

Roxanne Kimberly Moran

Professor Jay Sharping
Professor Boaz Ilan
Professor Erin Johnson
Professor Kevin Mitchell

Fall 2013

The thesis of Roxanne Kimberly Moran is approved:

Professor Boaz Ilan

Professor Erin Johnson

Professor Kevin Mitchell

Professor Jay Sharping

University of Calfornia, Merced
2013

To my parents, who have loved and supported me my entire life. Through every endeavor that I have ever decided to take on and any future endeavors that I will take on. I love you and you mean the world to me.

"Live as if you were to die tomorrow. Learn as if you were to live forever."
Mahatma Gandhi

Contents

List of Figures

Acknowledgments

Thank you to the people who I encountered that forever changed the way I learned-both academically and in life. Who worked with me extensively, never losing patience through the dozens of questions that I always had for you. You inspired me to be the same way when I had my own students to teach. You taught me that understanding the physical concepts was everything. Slogging through symbols and equations did not matter. That as long as I understood the physical picture, I had everything. True understanding and the world at hand. Thank you for all you have done for me. I would not have gotten as far as I have today without any of you. You inspired me as an undergraduate, a graduate student and in life. Thank you: Dr.Ching-Yao Fong, Dr. Randy Harris, Dr. Rodney Cole, Grant Acosta and Dr. Roland Winston. I am forever grateful to all of you.

Thank you to my dear friend, Francesca Ricci-Tam, who has made the journey along the way more bearable-both academically and personally.

Finally, thank you to my thesis committee: Dr. Boaz Ilan, Dr. Erin Johnson, Dr. Jay Sharping and my advisor Dr. Kevin Mitchell for working with me and helping me get this far.

Abstract

Dipolar Bose-Einstein Condensate Dynamics in A Chaotic Potential

by

Roxanne Kimberly Moran

Master of Science

in

Physics

University of California, Merced

2013

Professor Jay Sharping, Chair

Recent theoretical work has shown that short-range contact and long-range dipolar interactions of a Bose-Einstein condensate provide the stability needed for the formation of a two-dimensional soliton in a chaotic optical-dipole potential. However, inclusion of the dipole-dipole interaction causes the BEC soliton to deviate from the classical trajectories of the trapping potential and to instead follow trajectories given by an effective potential that is equal to the convolution of the external trapping potential and density profile of the BEC in the xy plane.

1.1 Introduction

Experimentally, the creation of solitary waves in AMO physics has been an area of interest, but the stability of such objects has made them a challenge to create in the laboratory [1]. Solitary waves are of optical interest because they may serve as an object that allows for experimental control [2]. It has been shown that dipolar Bose-Einstein Condensates (BECs) may provide the stability needed to form such solitary wave because they have atomic dipole-dipole interactions that act at long distances throughout the gas that are said to be nonlocal and nonlinear in behavior [2] [3]. It has been theorized that this anisotropy of the dipolar interactions and their ability to be "tuned" experimentally by using rotating magnetic fields is what provides the stability needed in a dipolar BEC for the formation of a solitary wave [1] [2].

In this thesis, we expand on the idea in Ref.[4] and use a "pancake shaped" dipolar BEC to create a 2D solitary wave in a chaotic potential, assuming confinement of the dipoles in the z-direction. As suggested by Ref. [1], we assume the tight confinement in the z-direction is due to an externally applied magnetic field. This tight confinement is necessary to prevent the attraction of the dipolar interactions' spins from causing the dipolar BEC to physically collapse in on itself. We also include repulsive s-wave scattering contact interactions in our model, which can be tuned experimentally by using Feshbach resonances [5].

The chaotic escape dynamics of a BEC in a chaotic potential was previously studied using the Gross-Pitaevskii model but not accounting for dipolar interactions [6] and is the motivation behind the study in this thesis. In the study done by Ref.[6], the BEC was found to follow the same trajectory as that of an ensemble of classical trajectories but with quantum interference fringes superimposed on the BEC [6].

Including attractive dipolar interactions in our study provided the stability that was needed to form a 2-dimensional solitary BEC structure. The dipolar interactions were able to counteract the repulsive s-wave scattering interactions and the inherent tendency of the dipolar BEC wave to disperse. These long-range dipolar interactions also dramatically enhanced the fractal structure in the dipolar BEC's escape-time dynamics and eliminated the interference fringes that were seen in the study done by Ref. [6].

1.2 Overview

1.2.1 General Concept Behind the Numerical Simulations

To model our dipolar BEC, we followed the approach used in Ref. [4] which was to start with the 3-dimensional Gross-Pitaevskii equation, reduce it to 2-dimensions and then use a Gaussian ansatz to numerically simulate the dipolar BEC's dynamics in the double-Gaussian potential. From there, we solve for the energy of the dipolar BEC a function of its widths in the xy plane, denoted by ρ and z-direction and then minimize the energy of the system. Our system having an energy minimum is what allows the BEC to form a 2D solitary structure in our chaotic potential. From the minimized energy equation, we can solve for equations that determine the strength that the contact and dipolar interactions need to have in order for the BEC to have the stability needed to form a 2D solitary wave. Once we have this relation, we can numerically simulate the dynamics of the dipolar BEC in the double-Gaussian potential and record its evolution and escape flux as functions of time.

1.2.2 Potential Energy Well

We start our simulations by placing the dipolar BEC in a double Gaussian potential well that has the following form:

$$V_{ext} = V(x,y) = V_1 e^{(\frac{x^2}{2\sigma_{1x}^2} - \frac{y^2}{2\sigma_{1y}^2})} - V_2 e^{(\frac{x-x^2}{2\sigma_{2x}^2} - \frac{y^2}{2\sigma_{2y}^2})} \tag{1.1}$$

where x and y refer to positions in the well and σ_{1x}, σ_{2x} and σ_{1y}, σ_{2y} represent the widths of the Gaussians in the x and y directions, respectively. The motivation behind using a chaotic potential comes from a preceding study done by Ref. [7], where the interest was to use cold atoms to create a chaotic system that would produce behavior similar to the chaotic ionization of a hydrogen atom when placed in parallel electric and magnetic fields and be able to image this self-similar behavior. Ref. [7] stated that these classical ionizing trajectories would show fractal self-similarity. Ref. [6] expanded on Ref.[7]'s study by using Schrödinger and Gross-Pitaevskii models to study these self-similar structures in a non-dipolar BEC. This thesis is an extension of the work done by Ref.[7] and Ref.[6] where we are looking for an enhancement of the self-similar structure seen in the escape-time dynamics of a dipolar BEC and observing how the dipolar BEC evolves in the chaotic potential as a function of time.

This double-Gaussian potential confines the BEC in the xy plane so that it is essentially 2-dimensional and "pancake shaped." The Gaussians overlap in such a way that a saddle is created between them, creating "left" and "right" portions of the well. Experimentally, overlapping Gaussians can be realized as an optical dipole trap and the tight confinement in the z-direction could be obtained by having a laser sheet intersect the two lasers that produce the overlapping Gaussians. As previously mentioned, we assume that an externally applied magnetic field in the z-direction aligns the magnetic dipoles' spins so that the dipolar BEC does not collapse in on itself.

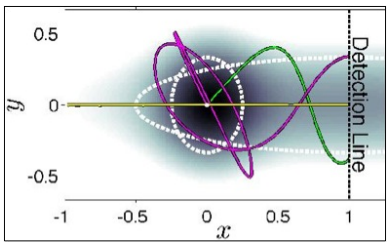

Figure 1: The dotted white lines outline the shapes of each of the Gaussian wells. One well is greatly elongated in the horizontal direction compared to the other. The depth of the well extends into the page. Any part of the BEC that crosses the "detection line" is considered never return to the potential well. The magenta and green curves represent trajectories that could result from exposure to this potential trap. Examples of classical trajectories are shown in magenta and green.

Once the dipolar BEC is placed in the center of the overlapping Gaussians and given an initial momentum in a particular direction, θ, which we call the "launch angle" we observe two quantities, the evolution of the dipolar BEC and the escape dynamics in the trapping potential, both as functions of time. We then compared our dipolar results to previous studies where non-dipolar BECs were simulated using Classical, Linear Schrödinger and Nonlinear Schrödinger models where the same quantities were observed and then compared to central trajectory data [6] [7].

1.3 Models

1.3.1 Present Study: Dipolar Model Using the Non-Local Gross-Pitaevskii Equation

As mentioned earlier in this thesis, we set out to model the dipolar BEC by starting with the 3-dimensional Gross-Pitaevskii equation:

$$i\hbar\frac{\partial}{\partial t}\Psi(\mathbf{r},t)=\left[-\frac{\hbar^2}{2}\nabla^2+V_{ext}+g|\Psi(\mathbf{r},t)|^2+\int d\mathbf{r}'V_d(\mathbf{r}-\mathbf{r}')|\Psi(\mathbf{r}',t)|^2\right]\Psi(\mathbf{r},t) \tag{1.2}$$

where the $-\frac{\hbar^2}{2}\nabla^2$ represents the kinetic energy of the system and V_{ext} represents the external trapping potential due to the double-Gaussian well which is again, given by:

$$V_{ext}=V(x,y)=V_1e^{(\frac{x^2}{2\sigma_{1x}^2}-\frac{y^2}{2\sigma_{1y}^2})}-V_2e^{(\frac{x-x^2}{2\sigma_{2x}^2}-\frac{y^2}{2\sigma_{2y}^2})} \tag{1.3}$$

$g|\Psi(\mathbf{r},t)|^2$ in Eqn. (1.2) represents the contribution of the short range, s-wave scattering interactions, where the contact interaction strength is given by $g=\frac{4\pi\hbar aN}{m}$. N is the number of particles in the BEC, m represents the mass and a is the s-wave scattering length. In the dipolar model, $a>0$, which corresponds to the fact that the short-range interactions are repulsive. The integral term, $\int d\mathbf{r}'V_d(\mathbf{r}-\mathbf{r}')|\Psi(\mathbf{r}',t)|^2$ accounts for the interaction energy due to the dipolar interactions and is given by:

$$V_d(\mathbf{r})=\frac{g_d(1-3cos(\theta)^2)}{r^3} \tag{1.4}$$

The distance between the dipoles is represented by $\mathbf{r}$. $g_d=\frac{\alpha Nd^2}{4\pi\epsilon_0}$ is the dipolar interaction strength, where ϵ_0 is the permittivity in vacuum. It is important to note that the dipolar interactions have a negative sign which corresponds to them being attractive and counteracting the repulsive contact interactions and the dispersive nature of the BEC. Experimentally, the sign of the dipolar interactions can be manipulated by using an externally applied magnetic field as previously mentioned. Also, note that the density of the dipolar BEC is normalized, $\int d\mathbf{r}|\Psi(\mathbf{r},t)|^2=1$. We then use the a Gaussian ansatz of the form:

$$\psi_0(\mathbf{r})=\frac{1}{\pi^{3/4}l_z^{3/2}L_\rho L_z^{1/2}}exp\left(-\frac{x^2+y^2}{2l_z^2L_\rho^2}-\frac{z^2}{2l_z^2L_z^2}\right) \tag{1.5}$$

to reduce the 3-dimensional Gross-Pitaevskii equation to an essentially 2-dimensional equation:

$$i\hbar\frac{\partial}{\partial t}\psi(\rho,t)=\left[\frac{-\hbar^2}{2m}\nabla_\rho^2+\frac{g}{\sqrt{2\pi}l_z}|\psi(\rho,t)|^2+\frac{4\sqrt{\pi}g_d}{3\sqrt{2}l_z}\int\frac{d\mathbf{k}_\rho}{(2\pi)^2}e^{i\mathbf{k}_\rho\cdot\rho}\tilde{n}(\mathbf{k}_\rho)h_{2D}\left(\frac{k_\rho l_z}{\sqrt{2}}\right)\right]\psi(\rho,t) \tag{1.6}$$

In Eqn. (1.5), $l_z=\sqrt{\frac{\hbar}{m\omega_z}}$ is the "thickness" of the BEC in the z-drection and L_ρ and L_z are dimensionless variational paramaters that correspond to the widths in the ρ plane and z- direction, respectively.

Solving for the energy of the BEC as a function of its widths in the ρ plane and z-direction, we obtain the following energy equation:

$$\frac{2E}{\hbar\omega_z} = \frac{1}{L_\rho^2} + \frac{1}{2L_z^2} + \frac{L_z^2}{2} + \frac{1}{\sqrt{2\pi}L_\rho^2 L_z \hbar\omega_z l_z^3}\left[\frac{g}{2\pi} + \frac{2g_d}{3} f\left(\frac{L_\rho}{L_z}\right)\right] \tag{1.7}$$

where $f(\kappa) = (\kappa^2-1)^{-1}[2\kappa^2 + 1 - 3\kappa^2 H(\kappa)]$ and $H(\kappa) = \frac{arctan(\sqrt{\kappa^2-1})}{\sqrt{\kappa^2-1}}$, $\kappa = \frac{L_\rho}{L_z}$.

Minimizing Eqn. (1.7) gives us the following equations:

$$1 + \frac{g}{(2\pi)^{3/2}\hbar\omega_z l_z^3} L_z\left[1 - \frac{2\pi}{3}\beta F\left(\frac{L_{\rho_z}}{L_z}\right)\right] = 0 \tag{1.8}$$

$$L_z = \frac{1}{L_z^3} + \frac{g}{(2\pi)^{3/2}L_\rho^2 L_z^2 \hbar\omega_z l_z^3}\left[1 - \frac{4\pi}{3}\beta G\left(\frac{L_\rho}{L_z}\right)\right] \tag{1.9}$$

$$F(\kappa) = (1-\kappa^2)^{-2}[-2\kappa^4 - 7\kappa^2 + 2 + 9\kappa^4 H(\kappa)] \tag{1.10}$$

$$G(\kappa) = (1-\kappa^2)^{-2}[-2\kappa^4 - 10\kappa^2 + 1 - 9\kappa^2 H(\kappa)] \tag{1.11}$$

$$\beta = \frac{g_d}{g} \tag{1.12}$$

Eqns. (1.8) and (1.9) allow us to determine the strength that g and g_d need to have with respect to one another to allow for the formation of a stable, 2-dimensional solitary wave. It is important to reiterate that our system having an energy minimum is what allows for formation of our 2D solitary wave.

$$\frac{2g_d}{3\sqrt{2\pi\hbar\omega_z l_z^3}} < 1 + \frac{g}{(2\pi)^{3/2}\hbar\omega_z l_z^3} < \frac{-4g_d}{3\sqrt{2\pi}\hbar\omega_z l_z^3} \tag{1.13}$$

Eqn. (1.13) is the relation between g and g_d determined by Ref. [4], which suggests $\beta = 0.12$. It is important to note that choosing $\beta = 0.12$ did not produce a stable 2D solitary structure in our simulations. So, we numerically simulated the dipolar BEC in the double-Gaussian potential until we found a relation between g and g_d that produced our 2D solitary wave. Though there is a difference between our simulations and Pedri and Santos' study in that we uses an external, double-Gaussian potential and Ref. [4] instead used a confining potential in the z-direction of the form $U = \frac{m\omega_z^2 z^2}{2}$, we do not fully understand the source of this discrepancy at this time, but plan on invesitgating it further in future work. From here, we were able to numerically simulate the dipolar BEC's evolution and escape-time dynamics in the double-Gaussian potential.

1.4 Preceding Studies: Concept of Each Model

There are three models from previous studies that we compared the results of our dipolar simulations to: the Classical [6] [7], Schrödinger [6] and Gross-Pitaevskii for contact interactions [6]. The double-Gaussian potential was used as the external potential in each of these simulations and each of these simulations' results were compared to that of the central trajectory. The key difference between these simulations and the dipolar simulation is that the dipolar simulation used an $\hbar$ value that was smaller than that which was used in the other simulations. This is an aspect we intend to address in future work as well.

1.4.1 Classical

The classical simulation involved launching individual particle trajectories at different values of the launch angle, θ and collectively observing the behavior of these trajectories to model the non-dipolar BEC [7]. The phase-space probability distribution used in this simulation was given by:

$$\rho(\mathbf{r},\mathbf{p}) = (\frac{1}{2\pi\sigma_r\sigma_p})^2 exp(\frac{-r^2}{2\sigma_r^2} - \frac{|\mathbf{p}-\mathbf{p_{c0}}|^2}{2\sigma_p^2}) \tag{1.14}$$

The position of the particle was represented by $\mathbf{r}$. σ_r and σ_p represent the standard deviations in position and momentum respectfully. $|\mathbf{p_{c0}}|^2$ reprsents the central momentum of the packet.

1.4.2 Schrödinger

The Schrödinger simulation is a linear, quantum mechanical model that treats the non-dipolar BEC as a wave, but does not account for the atomic interactions that occur within the BEC.

$$i\hbar\frac{\partial}{\partial t}\Psi(\mathbf{r},t) = \left[-\frac{\hbar^2}{2}\nabla^2 + V_{ext}\right]\Psi(\mathbf{r},t) \tag{1.15}$$

$\Psi(\mathbf{r},t)$ represents the state of the BEC, $-\frac{\hbar^2}{2}\nabla^2$ represents the kinetic energy of the system and $V_{external}$ represents the external potential due to the double-Gaussian potential.

1.4.3 Gross-Pitaevskii : Contact Interactions

The Gross-Pitaevskii model is the nonlinear version of the Schrödinger equation that allows us to account for the nonlinearity due to the contact interactions in our BEC. These local, s-wave scattering interactions are represented by the $g|\Psi(\mathbf{r},t)|^2$ term in the following equation:

$$i\hbar\frac{\partial}{\partial t}\Psi(\mathbf{r},t) = \left[-\frac{\hbar^2}{2}\nabla^2 + V_{ext} + g|\Psi(\mathbf{r},t)|^2\right]\Psi(\mathbf{r},t) \tag{1.16}$$

As in the dipolar case, the strength of the contact interactions is represented by $g = \frac{4\pi\hbar aN}{m}$ where a is the s-wave scattering length. It is important to note that $a < 0$ in the Gross-Pitaevskii contact interaction simulation, which corresponds to the short-range interactions being attractive to counteract the natural tendency of the BEC to disperse. This differs from the sign that the

contact interactions have in our Gross-Pitaevskii dipolar simulation, where $a > 0$ and the contact interactions are repulsive, but the dipolar interactions are attractive. N is the number of particles in the BEC and m represents the mass.

1.5 Results

1.5.1 BEC Evolution in the Potential Energy Well

One of the results that we looked at was the behavior of the BEC in response to the double-Gaussian potential as a function of time. We observed whether the BEC lost its shape by either collapsing in on itself or expanding to the point of exploding or kept its shape, thereby remaining intact and forming a 2-dimensional solitary structure. We then compared the trajectory that the dipolar BEC followed to the path that the central trajectory followed in the double-Gaussian potential and this is what is denoted by the white curve in Fig.2.

We then contrasted the dipolar comparison to the central trajectory data with the non-dipolar BECs' comparisons to the central trajectory data and that is what is shown in Fig.2. Escape-rate versus time plots are at the end of each simulation's sequence in Fig.2. The peaks in these escape-rate plots correspond to the time at which most of the BEC escapes the potential well, whereas the black vertical bar in each plot corresponds to the time that it takes for the central trajectory to leave the well.

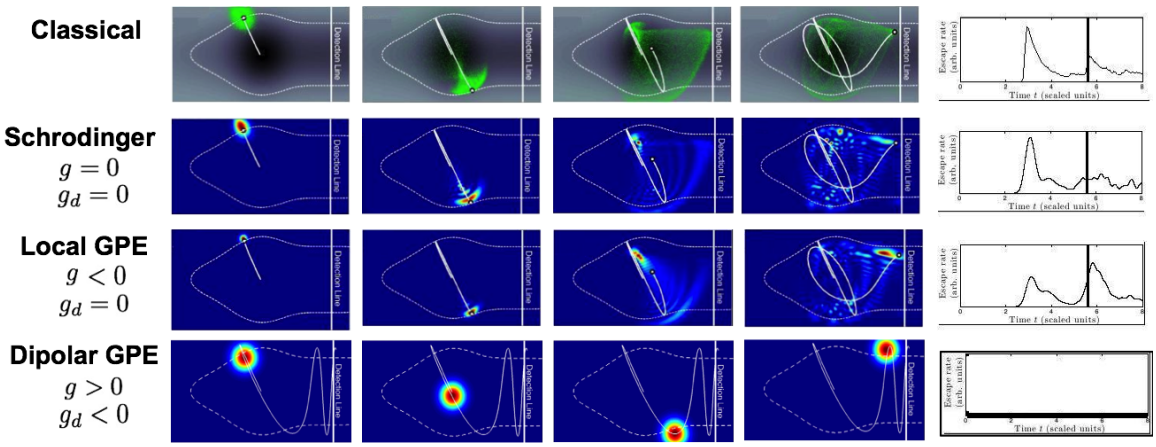

Figure 2: BEC evolution as a function of time for each of the four models: Classical, Schrödinger, Gross-Pitaevskii with only contact interactions, labeled as "Local GPE," and Gross-Pitaevskii with contact and dipolar interactions, labeled as "Dipolar GPE." The white curve in each of the frames represents the central trajectory's evolution. The black and white images at the end of each simulation's sequence is a plot of BEC flux as a function of time. In each simulation, the largest peak represent when most of the BEC has escaped the trap. The solid black vertical bar represents the time at which the central trajectory escapes the potential well.

1.5.2 Dipolar

The dipolar BEC, depicted in the fourth row of Fig.2, started out as a 2D solitary wave and retained its shape throughout the entire simulation. However, the dipolar BEC's trajectory differed from that of the central trajectory, which is seen by the dipolar BEC's white curve differing

from the white curve that is seen in the first three rows of Fig.2. The dipolar BEC packet is also noticeably smaller than the BECs in the other simulations that are shown in Fig.2. This is a result of the smaller $\hbar$ value that was used for the dipolar BEC that was mentioned previously. The dipolar escape flux plot does not have any peaks denoting when the dipolar BEC leaves the well or a vertical bar corresponding to the central trajectory. This is because for the particular angle for which the BEC evolution is depicted in Fig.2, $\theta = 2.04$, the dipolar BEC does not escape the trapping potential. This corresponds to being at the inside edge of an icicle on the escape-time plot, which will be elaborated on in the "Escape-time Dynamics" section of this thesis.

1.5.3 Classical

In the classical simulation, shown in the first row in Fig.2 the non-dipolar BEC started to disperse in the second frame from the left and did not recover, but its trajectory did coincid with the central trajectory's. However, most of the classical BEC escaped the well at a different time from the central trajectory. This can be seen by the large peak being at $t = 2.9$, not coinciding with the black vertical bar in the escape-rate versus time plot at $t = 6$ at the end of the first row in Fig. 2.

1.5.4 Schrödinger

In the Schrödinger simulation in the second row of Fig.2, we see that the BEC starts to disperse by the second frame also does not recover from this dispersion. Inteference fringes are seen in the Schrödinger simulation which is a result of the fact that the Schrödinger equation models the BEC as a wave. The interference fringes correspond to the wave intefering with itself. Most of the Schrödinger BEC escapes at $t = 3$ in the escape flux plot, still differing from the central trajectory's time of escape at $t = 6$.

1.5.5 Gross-Pitaevskii: Local

In these BEC simulations, $\hbar$, corresponds to the width of the BEC. Though, the Classical, Schrödinger and Gross-Pitaevskii Contact Interaction models all use the same value of $\hbar$, the contact interactions in the Gross-Pitaevskii Contact Interaction model hold the packet together, which is why it looks smaller than the Classical and Schrödinger BECs in Fig.2. Interference fringes are also seen in this model because the BEC is still being treated as a wave and can still interfere with itself. In the escape rate plot, most of the BEC escapes at time $t = 7$ which is closest to the time that the central trajectory escapes at $t = 6$.

1.6 Escape-Time Dynamics of the BEC

The other result that we looked at was the escape-time dynamics, which involved plotting the amount of BEC that escaped the potential well, which we called "flux," as a function of time for different launch angles from $\theta = 0$ to $\theta = \pi$. The dipolar BEC's escape-time data was then compared to central trajectory's escape-time data for a non-dipolar BEC, modeled using just the central trajectory, which can be seen in Fig.3, as the yellow icicles. This comparison was then contrasted with the Classical, Schrödinger and Gross-Pitaevskii Contact Interactions' models' comparisons to the central trajectory data.

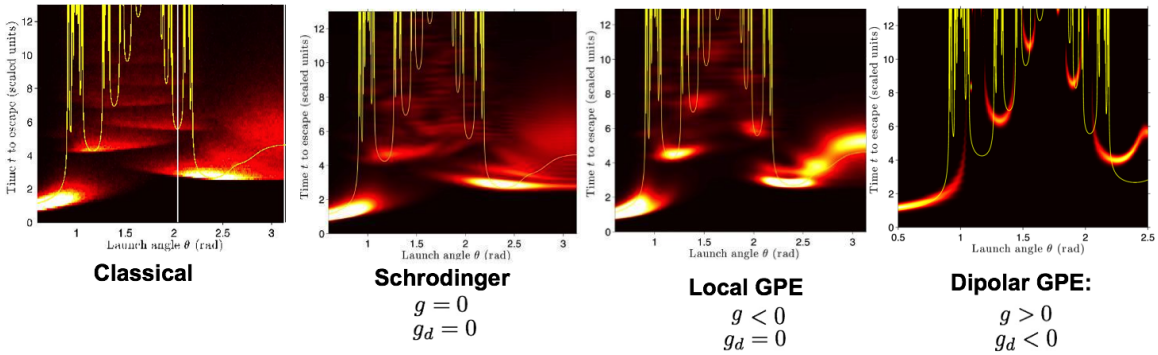

Figure 3: Escape-time plots for the Classical, Schrödinger, Gross-Pitaevskii Contact Interaction and Gross-Pitaevskii Dipolar Interaction models. The range of θ values from 0 to π, that the BEC was launched at is along the horizontal axis and the amount of time that it took for the BEC to escape the potential is on the vertical axis. The intensity of the coloration that varies from bright white to red to black in the graphs, reflects the amount of flux that escapes the trapping potential. Bright coloration represents a large amount of flux whereas the dark coloration indicates a smaller amount of flux. Plotted in yellow is the escape-flux as a function of time for the central trajectory. This graph should be read vertically. For example, let us look at the Classical Escape-Time Plot. Choose one value of θ along the horizontal axis, let's say $\theta = 1$ and follow the time-scale on the vertical axis from $t = 0$ to $t = 12$. At $t = 0$ for $\theta = 1$, we see black coloration in the figure. This means that none of the BEC has escaped the well yet. But, if we look at $t = 1$ for $\theta = 1$, we see bright coloration, which corresponds to a high intensity and therefore, large amount of BEC flux that has left the potential well at $t = 1$. If we look at $t = 2.2$, we see a darker, red coloration which indicates that not as much BEC flux has left the potential compared to $t = 1$ for example.

1.6.1 Dipolar

The Dipolar Gross-Pitaevskii escape-time plot has the sharpest fiery icicles because it is able to remain a wave packet and form a 2D solitary structure. However, the locations of the dipolar icicles are "shifted" and do not coincide with the bottoms of the yellow icicles, which correspond to the escape flux of the central trajectory. The region inside a fiery icicle corresponds to the BEC being inside the chaotic potential. Black regions on the escape-time plot mean that no BEC flux has left the trapping potential, so those areas correspond to times when the BEC is still "rattling around" in the potential well.

1.6.2 Classical

In the classical case, the fiery regions are blurred but the locations of the brightly shaded regions correspond to the bottoms of the central trajectory's icicles. The blurring is due to the fact that individual particle traejctories were used in the Classical simulation.

1.6.3 Schrödinger

The bright fiery regions are blurred, but still coincide with the locations of the bottom of the central trajectory's icicles. Resolution is improved compared to that which was seen for the Classical case. Interference fringes appear in the BEC and are result of the BEC being treated as a wave and interfering with itself.

1.6.4 Gross-Pitaevskii Contact Interactions

Contact interactions enhance the self-similar structure which is seen by the sharpening of the fiery regions, compared to the blurring that we saw in the Classical and Schrödinger cases. Interference fringes in the BEC are still present as a result from treating the BEC as a wave. The Gross-Pitaevksii Contact Interaction icicles also coincide better with the bottoms of the central trajectory's icicles.

1.6.5 Interpetation of BEC Evolution and Escape-Time Results

The comparison of the dipolar simulation to the Classical, Schrödinger and Gross-Pitaevskii simulations leaves us with the question of why the dipolar BEC's trajectory and escape-time data in the double-Gaussian potential differs from the central trajectory's which was not the case for the other three simulations. To understand the reason behind this difference in results, let us consider the following. Two of the simulations, the Classical and Schrödinger models, did not account for atomic interaction energies and two of them did, the Gross-Pitaevskii Contact Interaction and Gross-Pitaevskii Dipolar Interaction Models. However, the Gross-Pitaevskii Contact Interaction model still produced a BEC that followed the central trajectory's evolution in the double-Gaussian potential and has fiery icicles in its escape-time plot that more or less coincided with the locations of the bottom of the central trajectory's icicles in Fig.2 and Fig.3, respectively. The factor that is present in each of the simulations that has an effect on both the evolution and escape dynamics as functions of time of both the dipolar and non-dipolar BECs is the externally applied potential. This leads us to asking if the external potential that the dipolar BEC experiences is different from that experienced by the non-dipolar BECs. Referring back to Fig.2, the non-dipolar BECs started at the center of the potential well and dispersed not too long after being given an initial momentum. The dipolar BEC remained intact as a 2D solitary structure throughout the entire simulation, thereby experiencing more than just the value of the external potential near the center of the well. The dipolar BEC instead experienced an average of the external potential as it moves throughout the well, which we call an effective potential, V_{eff}.

$$V_{eff} = V_{ext} * |\psi(x,y)|^2 \tag{1.17}$$

where V_{ext} represents the external potential that our dipolar BEC is exposed to in the Gross-Pitaevskii Dipolar simulation and $\psi(x,y)$ is the wavefunction of the dipolar BEC in the xy plane. So the external potential energy that the dipolar BEC is exposed to, is just the convolution of the externally applied potential and the density profile of the dipolar BEC in the ρ plane.

Fig. 4 is an enhanced view of dipolar simulation's Escape-Time Plot and the important feature to note is that the white icicles correspond to a trajectory for the dipolar BEC that was simulated using the V_{eff} from Eqn. 1.17. Unlike the central trajectory's icicles, the effective potential's icicles "match up" with fiery icicles of the dipolar BEC's escape-time data.

1.7 Conclusion

In summary, attractive dipolar interactions were able to counteract the repulsive s-wave scattering interactions and the natural tendency of a wave to disperse in a chaotic potential, thereby allowing for the formation of a 2D solitary BEC structure. It was by keeping the dipolar BEC's shape intact that the anisotropic dipolar interactions were able to dramatically enhance the resolution of self-similar fractal structures seen in the escape-time data compared to that which was seen in previous models. It is because inclusion of the dipolar interactions allowed for an energy minimum

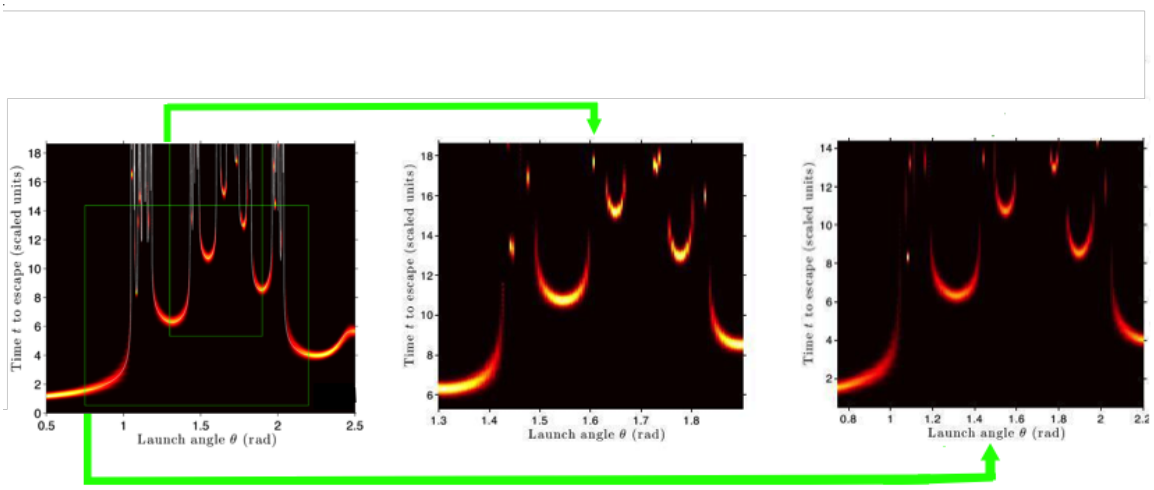

Figure 4: Zoomed in image of the Escape-Time Plot for the Dipolar BEC Simulation. The white icicles were determined by numerically simulating the dipolar BEC in the effective potential, V_{eff}.

in our BEC system that the dipolar BEC was able to be stable and form a 2D solitary wave. The resulting 2-dimensional solitary wave's trajectory while in the trapping potential was not strictly due to the external potential of the well, but the convolution of the external potential and the density profile of the BEC wavepacket in the ρ plane.

Future work will include revisiting $\beta = 0.12$ not producing a stable, 2D solitary wave in our dipolar simulations and running another dipolar BEC simulation with an $\hbar$ value equal to that which was used in the Classical, Schrödinger and Gross-Pitaevskii non-dipolar simulations.

References

[1] I. Tikhonenkov, B.A. Malomed and A. Vardi, Phys. Rev. Lett **100**, 090406 (2008);

[2] V.M. Lashkin, Phys. Rev. A **75**, 042607 (2007).

[3] I. Tikhonenkov, B.A. Malomed and A. Vardi, Phys. Rev. Lett **100**, 090406 (2008);
S. Yi and L. You, Phys. Rev. A **61**, 041604 (2000);
S. Yi and L. You, Phys. Rev A **66**, 013607 (2002);
K. Goral, K. Rzazewski, and T. Pfau, Phys. Rev. A **61**, 051601 (2000);
L. Santos *et al.*, Phys. Rev. Lett. **85**, 1791 (2000);
K. Goral and L. Santos, Phys. Rev. A **66**, 023613 (2002);
L. Santos, G.V. Shlyapnikov, and M. Lewenstein, Phys. Rev. Lett **90**, 250403 (2003).

[4] P. Pedri and L. Santos, Phys. Rev. Lett. **95** ,200404 (2005)

[5] F. Kh. Abdullaev *et al.*, Phys. Rev. Lett. **90**, 013605 (2003);
H. Saito and M. Ueda, Phys. Rev. Lett. **90**, 040403 (2003);
G.D. Montesinos, V.M. Perez-Garcia, and H. Michinel, Phys. Rev. Lett. **92**, 133901 (2004); M. Matuszewski *et al.*, Phys. Rev. Lett. **95**, 050403 (2005).

[6] K. A. Mitchell and B. Ilan, Phys. Rev. A **80**, 043406 (2009).

[7] K.A. Mitchell and D.A. Steck, Phys. Rev. A. **76**, 031403(R) (2007)

[8] T. Lahaye, C. Menotti, L. Santos, M. Lewenstein, and T. Pfau, The Physics of Dipolar Bosonic Quantum Gases, Rep. Prog. Phys. 72 (2009) 126401 (41pp).

[9] C.J. Pethick and H. Smith, *Bose-Einstein Condensates in Dilute Gases* (Cambridge University Press, Cambridge, 2008).

[10] L.P. Pitaevskii and S. Stringari, *Bose-Einstein Condensation* (Oxford University, New York, 2003).

[11] Jianke Yang, *Nonlinear Wave in Integrable and Nonintegrable Systems* (SIAM 2010)